Title
Quantifying Optimal Columellar Strut Dimensions for Nasal Tip Stabilization After Rhinoplasty via Finite Element Analysis

Journal
Facial Plastic Surgery & Aesthetic Medicine, 18(3)

ISSN
2689-3614

Authors
Gandy, Jessica R
Manuel, Cyrus T
Leary, Ryan P
et al.

Publication Date
2016-05-01

DOI
10.1001/jamafacial.2015.2261

Published in final edited form as:

JAMA Facial Plast Surg. 2016 May 01; 18(3): 194–200. doi:10.1001/jamafacial.2015.2261.

Quantifying Optimal Columellar Strut Dimensions for Nasal Tip Stabilization After Rhinoplasty via Finite Element Analysis

Jessica R. Gandy, BS, **Cyrus T. Manuel, BS**, **Ryan P. Leary, MD**, and **Brian J.F. Wong, MD, PhD**

School of Medicine, University of California, Irvine (Gandy, Leary, Wong); Beckman Laser Institute and Medical Clinic, University of California, Irvine (Gandy, Manuel, Leary, Wong); Department of Otolaryngology–Head and Neck Surgery, University of California, Irvine, Orange (Wong)

Abstract

IMPORTANCE—The contribution of columellar strut grafts (CSGs) to nasal tip support has not been determined via structural mechanics. Optimal graft dimensions have yet to be objectively determined.

OBJECTIVES—To use a finite element model (FEM) of the human nose to (1) determine the effect of the CSG on nasal tip support and (2) identify how suture placement contributes to tip support.

DESIGN, SETTING, AND PARTICIPANTS—A multiple-component FEM of the human nose consisting of bone, skin/soft tissue, and cartilage was rendered from a computed tomographic scan. Then, CSGs of varying sizes were created, ranging from 15 × 4 × 1 mm to 25 × 8 × 1 mm, and placed in the model between the medial crura. Two FEMs were constructed for each strut size: (1) CSGs that were physically attached to the nasal spine, medial crura, and caudal septum and (2) CSGs that were not in direct contact with these structures and free to move within the soft tissue. A control model was also constructed wherein no graft was placed.

Corresponding Author: Brian J.F. Wong, MD, PhD, Beckman Laser, Institute and Medical Clinic, University of California, Irvine, 1002, Health Sciences Rd, Irvine, CA 92612 (bjwong@uci.edu).

Conflict of Interest Disclosure: None reported.

Previous Presentation: This study was presented as a podium presentation at the American Academy of Facial Plastic and Reconstructive Surgery International Symposium; April 29, 2014; New York, NY.

Additional Contributions: We thank Allen Foulad, MD, who was instrumental in this study's inception and organization. Dr Foulad received no compensation for his contributions.

Disclaimer: Dr Wong is associate editor of *JAMA Facial Plastic Surgery*, but he was not involved in any of the decisions regarding review of the manuscript or its acceptance.

Author Contributions: Dr Wong had full access to all of the data in the study and takes responsibility for the integrity of the data and the accuracy of the data analysis.
Study concept and design: Gandy, Manuel, Leary, Wong.
Acquisition, analysis, or interpretation of data: Gandy, Manuel, Leary, Wong.
Drafting of the manuscript: Gandy, Manuel.
Critical revision of the manuscript for important intellectual content: Manuel, Leary, Wong.
Obtained funding: Wong.
Administrative, technical, or material support: Manuel, Leary, Wong.
Study supervision: Leary, Wong.

MAIN OUTCOMES AND MEASURES—Nasal tip support for each model was assessed, and the resultant distribution of von Mises stress, reaction force, and strain energy density with respect to the alar cartilages were calculated.

RESULTS—Compared with the control, the reaction force increased with increasing strut volume, while the strain energy density (calculated over the alar cartilages) generally decreased with increasing CSG volume. Simulations with struts that had suture attachments along the entire length of the graft generated a larger reaction force than the models without any suture attachments. Models with anteriorly placed sutures generated reaction forces similar to that of the fully sutured model, whereas the models with posterior sutures showed reaction forces similar to the fully disconnected model.

CONCLUSIONS AND RELEVANCE—Insertion of CSGs does effect the amount of force the nasal tip can withstand post rhinoplasty. Moreover, anteriorly placed sutures incur reaction forces similar to struts that are fully connected to the alar cartilage. Thus, our simulations are congruent with clinical practice in that stability increases with graft size and fixation, and that sutures should be placed along either the entire CSG or the anterior most portion for optimal support.

LEVEL OF EVIDENCE—NA.

In rhinoplasty, one of the most important and difficult determinants of long-lasting positive outcomes has been the maintenance of nasal tip support. Anderson[1] formed the foundation of what we understand today about nasal tip dynamics with the tripod concept. The theory of nasal tip dynamics was further enhanced by the work of Tardy and Brown,[2] who grouped the nasal tip support structure into major and minor categories. A major component of maintaining nasal tip support is the columellar structure, which is inevitably compromised in most rhinoplasty operations. It is now common-place among facial plastic surgeons to reconstruct the columella after rhinoplasty surgery.[3] One such method includes the insertion of a columellar strut graft (CSG), which is usually constructed from autologous septal cartilage, although conchal and costal cartilage may also be used. The cartilage used for the graft is cut into a rectangular segment with dimensions complementing the patient anatomy prior to placement between the medial crura along the caudal edge of the septum and abutting the nasal spine.

The CSGs are a critical component of open structure rhinoplasty and are thought to be essential to maintain tip support. In clinical practice, strut graft dimensions are derived from the size of available cartilage tissue and the surgeon’s intuition and clinical experience rather than objective analysis. Previous studies have demonstrated that proper placement of CSGs provides a statistically significant increase in nasal tip support that is further augmented with intracrural fixation.[4–7] However, optimal graft dimensions and ideal intracrural suture placement have not been objectively analyzed or reported. Conducting prospective randomized clinical trials to evaluate rhinoplasty outcomes is nearly impossible because of ethical limitations, wide variations in surgical techniques, differences in patient anatomy, and the necessity to produce an optimal result for every patient. Thus, most of the clinical research in facial plastic surgery to date has relied on expert opinion and retrospective data.[8] Naturally, owing to these limitations, computational modeling may provide insight into the

mechanical consequences of various routine surgical interventions and help inform clinical practice.

The finite element model (FEM) has been used to study the mechanics of several structural organs including the joints, spine, middle ear, and nasal septum to investigate load distribution and forces encountered during manipulation.[9–16] Previous work by Manuel et al[17] aimed to construct an anatomically accurate multicomponent FEM of the nose consisting of 3 soft-tissue components, bone, cartilage, and skin. Shamouelian et al[18] further demonstrated that this FEM can be used to analyze the structural mechanisms behind nasal tip support.

In the present study, we used finite element analysis to examine how graft size, shape, and connectivity (suture configuration) to the medial crura affect nasal tip support. Palpation, a routine part of the physical examination performed to evaluate nasal tip support, was simulated in the model using static loads whereby the nasal tip was depressed 5 mm. The resultant simulations provide information on how CSGs influence nasal mechanics and may contribute to nasal tip support.

Methods

Construction of the Columellar Strut Grafts

This study was approved by the institutional review board at University of California, Irvine; patient written informed consent was waived. The FEMs were constructed from a high-resolution computed tomographic (CT) scan of a single patient using a series of software packages, as previously described by Manuel et al.[17] Briefly, soft tissue and bone were rendered using Mimics (Materialise; Materialise NV). Computer-aided design software (Autodesk 3DS Max; Autodesk Inc) was used to generate patient-specific and anatomically correct septal, upper lateral, and the lower alar cartilages, and these data were then imported into Mimics. This original model served as our control for comparison with columellar strut models. The columellar strut was rendered in Mimics using orthogonal views in the CT scan as a guide, and neighboring cartilages were adjusted to accommodate the strut. Mesh generation and assembly were performed in 3-Matic (Materialise NV) and then imported into COMSOL Multiphysics (COMSOL Inc), where material properties and boundary conditions were assigned. An example of the model can be seen in Figure 1.

A total of 10 FEMs were created with different strut graft dimensions. Each CSG was inserted between the medial crura of the lower alar cartilage, and its dimension was adjusted using the Mimics 3-dimensional editing function. The length and width varied, while the thickness remained constant at 1 mm (Table); the smallest graft measured 15 × 4 × 1 mm, and the largest was 25 × 8 × 1 mm.

Approximating Suture Placement

Columellar strut grafts are typically inserted between the medial crura and secured with at least 2 sutures that are placed along the length of the columellar strut. To study the dependence of nasal recoil on suture placement, we fashioned 4 variations of the 25 × 8 × 1-mmstrut graft model: a fully connected strut, an anterior connected strut (ie, toward the nasal

tip), a posterior connected strut (ie, toward the nasal spine), and a fully disconnected strut (ie, strut placement without any sutures). Connectivity simulating suture placement was also achieved using the Mimics 3-dimensional editing function by deleting or adding voxels between the medial crura and caudal septum (Figure 2). For the purposes of this study, we define reaction force as the force that opposes nasal tip compression. The mechanical properties previously defined by the intercartilaginous connection between the crura and the caudal septum were redefined as the soft-tissue material properties.

Simulation of Tip Compression

Finite element analysis of the models was performed in COMSOL Multiphysics. Linear elastic and isotropic properties were assigned to skin, cortical bone, cartilage, and columellar strut model components. The material properties of skin, bone, and cartilage were obtained from the literature and are referenced by Manuel et al (Table 1).[17] To simulate nasal tip displacement, an approximate 10-mm^2 surface on the tip of the nose was prescribed a displacement of 5 mm in the posterior direction.

Recoil Force, von Mises Stress, and Strain Energy Density

Von Mises stress distribution, along with the model strain, was calculated for each model to analyze the strut and surrounding tissue under nasal tip compression. Von Mises stress is a scalar value that combines the normal and shear stresses under a complex 3-dimensional loading condition.

In addition to identifying load-bearing regions on nasal tip support structures, we also determined the reaction force of the entire model for all models. The nasal tip recoil force, which is estimated subjectively during the physical examination, was calculated by integrating the uniaxial reaction force (the force that opposes the nasal tip compression) over cartilage components positioned against bone.

Strain energy density, which is the energy required to restore the material to its original shape, was calculated over the alar cartilage components and septum minus the entire strut volume. It is a scalar value that reflects energy storage in a structure following deformation. The insertion of a strut was accomplished by reassignment of tissue mechanical properties from soft tissue to that of cartilage. For example, in cases where a large strut would overlap the medial crura, the medial crura were made proportionally smaller. In general, it would be expected that a larger CSG would absorb more of the energy from nasal tip depression, and the nasal cartilages would absorb less. In contrast, one would expect the control to display a higher strain energy density because the nasal cartilages would absorb most of the energy.

Data were analyzed to establish 2 main points: (1) to determine if the addition of a strut differs from the control (no strut) and (2) to determine if varying the suture attachments of the strut to the medial crura—attachments along entire length of the strut, anterior attachments only, posterior attachments only, and fully disarticulated—makes a difference in overall nasal tip reaction force.

Results

Effect of Strut Size on Recoil Force and Strain Energy Density

In terms of nasal tip compression, the placement of a strut adds to nasal tip recoil force compared with the control with no strut graft (Table 2). As previously reported by Manuel et al,[17] the load-bearing regions of the control are concentrated at the alar, upper alar, and septal cartilages. Similarly, models with struts show load-bearing regions in the same areas, including the anterior portion of the strut. The reaction force increased with increasing strut volume, while the strain energy density appeared to generally decrease with increases in strut volume (Table 2).

Effect of Strut Attachments on Recoil Force

A 25 × 8 × 1-mm strut with attachments along the entire length of the graft generated a relatively larger recoil force than the fully disconnected models (difference of 0.2 N). Interestingly, the models with anterior attachments generated reaction forces similar to those of the fully connected model, while the models with posterior attachments only showed reaction forces similar to those of the fully disconnected model(Table 2).

Effect of Strut Attachments: von Mises Stress

Surface plots of the von Mises stresses indicate that the load-bearing regions of nasal cartilages were concentrated in the medical crura, anterior nasal strut, and inferior upper lateral cartilages. Oblique and base views of the cartilage are shown in Figure 3, with the bone, skin, and soft-tissue components fully transparent. The areas of red indicate high amounts of stress, while the areas in blue indicate low amounts of stress. In the base of view, the highest amount of stress was concentrated in the patient's right medial crus. The peak stress for the control was 270 kPa, and the peak stress for the model with 25 × 8 × 1-mmfully connected CSG was 261 kPa.

Compared with no strut, the fully connected strut models generated larger amounts of stress (more areas of red) at the nasal tip, specifically the anterior most portions of the alar, upper alar, and septal cartilages (Figure 3). In all models, the posterior aspect of the nasal septum was not at all affected by the depression (areas of blue). Regarding von Mises stress distribution, anteriorly connected struts generated larger areas of stress than posteriorly connected and disconnected struts (Figure 4). In addition, the anteriorly connected strut model predicted a concentration of stress (red) (Figure 4C) toward the nasal tip compared with the posteriorly connected model, which showed a more diffuse stress (red) pattern (Figure 4D). These results are consistent with recoil force values in that the posteriorly connected and disconnected struts can generate less recoil force than the anteriorly connected and fully connected struts and thus cannot withstand as much stress.

Finally, in evaluating the stress incurred on the strut itself, we found that the postnasal tip depression demonstrated von Mises stress distributions consistent with the results obtained from the oblique and base cartilage views. Appropriately, the anterior-most portion of the strut underwent the most amount of stress (Figure 4). Furthermore, the model with the

anteriorly connected strut produced a higher recoil force than the fully disconnected and posteriorly connected models (difference of 0.16 N).

Discussion

While the efficacy of the columellar strut has been clinically established for years, the actual mechanical impact of CSG placement on nasal tip stability has received little scrutiny and has been neither modeled nor simulated using actual patient geometry. In 2001, Beaty et al[4] quantified the changes in strength of nasal tip support associated with the insertion of CSG using a tensiometer to measure tip recoil and demonstrated that a CSG provided a 40% increase in nasal tip support in the vector along the columella that was further strengthened by intracrural sutures. Furthermore, in 2010, Dobratz et al[5] quantified the strength of various methods of columellar reconstruction in cadavers and demonstrated that the medial crural attachment to the caudal septum is crucial to maintain optimum support of the nasal tip. Computational models simulating this maneuver, or for that matter any structural rhinoplasty graft, are lacking. Our group has simulated other common maneuvers in rhinoplasty surgery, but we have focused on simulating the effects of cartilage resection, which is more simple to render in silico.[15–18] Computational models allow parametric analysis that provides insight into how changes inform factor and geometry may alter mechanical stability. Using a FEM in the present study, we estimate the reaction force (tip recoil force) and strain energy density of various CSG designs in response to tip depression, with the aim of understanding how changes in CSG geometry and attachment to the medial crura affect support.

Reaction force was calculated and observed to increase with strut volume (cubic millimeters), which is intuitive, given that the FEM is a linearly elastic model. When comparing the smallest CSG with the largest, we found that the reaction force generally increased with graft volume and then reached a plateau. With regard to strain energy density, a general pattern was observed: as strut volume increased, strain energy density decreased. The strain energy density is the 3-dimensional analogue to the energy under a stress strain curve. In 3 dimensions, this is more complex in definition but still is a scalar value that reflects energy storage in a structure following deformation. We are limited in this study in that the columellar geometry was not varied, and the total volume of soft tissue and cartilage in this region was constant for each case evaluated. The insertion of a strut was accomplished by reassignment of tissue mechanical properties from soft tissue to that of cartilage. In cases where a large strut would overlap the medial crura, the medial crura were made proportionally smaller. This is in contrast to actual surgical conditions, where columella volume increases as does total cartilage content. This is an intrinsic limitation of the present model; the alternative would require a challenging rerendering of the entire nasal columellar complex, which is beyond the scope of this study.

With regard to reaction force, the data summarized in Table 2 suggest an optimal strut size and volume and point to a potential saturation threshold at which a larger strut may actually be less effective due to limitations with the patient’s anatomy and nose size. In this study, the 25 × 8 × 1-mmstrut accounts for the largest reaction force. Larger grafts in this FEM would exceed real world clinical graft dimensions and thus were not investigated, though larger grafts would likely produce modest increments, if any, in recoil force. Obviously, these

outcomes are specific to this FEM only, and different patient models may result in the accommodation of larger graft sizes. In both patients and a FEM, overall nasal tip size limits graft size as well.

We also found that suture placement is just as important a factor as strut size—a concept that has not been examined previously to our knowledge. Securing the strut to the medial crura with a suture is the most important part of the strut graft insertion process. To simulate differences in suture technique, we created 4 simple models with different types of attachments to the medial crura. The reaction force generated by the fully connected models (the CSG in direct contact with the medial crura) was larger than the reaction force generated by the fully disconnected struts (CSG fully disconnected from the medial crura); this is as expected. Analysis of the partially connected models indicates that it is most important to suture the proximal/anterior section of the CSG to the medial crura (Table 2). However, placement of additional sutures along the entire segment of the strut to the alar cartilage will further enhance stability. This has been observed in mechanical studies of polydioxanone plates secured to cartilage grafts as well.[19]

Regardless, the FEM used in the present study has not been validated experimentally, and the quantitative values produced in simulation must be interpreted with caution. Validation using a physical model of the nose is currently an active focus of our research group. Still, this phenomenological model and approach has the potential to teach and inform about structural behavior during rhinoplasty and may be of significant value when used to examine structural framework changes where the distributions of stress and strain are not as readily predictable. Over the past several decades, new techniques in open structure rhinoplasty have evolved and become more widely adopted.[20,21] However, the impact of these new maneuvers in many cases is unclear, and clinical experience may be limited. Using an FEM may help guide surgeons in how to best select and potentially optimize their surgical approach.

The present study is a foundation on which future studies can build and improve. Some limitations of the study include the fact that the FEM assumes linear elastic properties for soft tissues and cartilage. Real tissues are viscoelastic, and there is limited information on the mechanical properties of nasal and facial tissues. Furthermore, the individual components of the model, such as skin, bone, cartilage, soft tissue, and the CSG were created de novo using a computer software program. Thus, manual error could account for variations and decrease accuracy. Also, this model assumes all soft-tissue components to be the same. For example, the subcutaneous, adipose, ligamentous structures, and fascia are not separate entities in the FEM. This may detract from the model’s ability to fully replicate what is happening in an actual human patient. Furthermore, this model is based on the CT scan of a single patient with a caudal septal deviation. Thus, these results, such as specific values for stress, strain, and reaction force are tailored to this particular patient, and any generalization to leptorrhine or platyrrhine noses must be performed with prudence. Nonetheless, the general trends should remain true independent of differences in anatomy.

Finally, the relative changes between the larger and smaller struts, as well as differences in suture placement, while present in this model, may or may not be significant in clinical

practice with human models. In general, the decision whether to place a strut is a clinical one and is based on years of clinical practice. Thus, further studies are warranted to determine the significance of strut size and suture placement in human noses. This may be difficult to study clinically, and thus the present model allows for potential extrapolation and translation into clinical practice. Ultimately, this study's model is a starting point on which to build a more precise, all-encompassing model in the future.

It is our long-term objective to eventually use this approach to enhance and further individualize rhinoplasty. This is the first of many studies in which we plan to examine grafting and structural rhinoplasty using finite element analysis. Just as in oncology, where patient-specific molecular therapies are tailored and refined for each individual, in rhinoplasty, FEM scan be used to accomplish this task for many aesthetic procedures. Presently in rhinoplasty, surgeons can use morphing software to simulate results preoperatively, and this capability has enhanced and improved outcomes in ways that traditional photography, ink, and tracing paper never could. Integrating FEM into the current preoperative simulations may not only provide better predictability of overall results, but will also give surgeons a better sense of the structural outcomes that accompany surgical maneuvers. Surgeons will be able to analyze the effects of different grafts, suture techniques, and other surgical elements under different types of loading situations for each individual patient, predict stress distribution in response to displacement, loads, gravity, or the forces of scarring, and then calculate potential steady-state changes in nasal geometry.

Conclusions

Using FEM, we found that insertion of CSGs strengthens the nose by increasing the reaction force when it is palpated post rhinoplasty. Moreover, anteriorly placed sutures incur reaction forces similar to struts that are fully connected to the alar cartilage. Thus, our simulations are congruent with clinical practice in that stability increases with graft size and fixation and sutures should be placed along either the entire CSG or the anterior-most portions to the alar cartilages for optimal tip support.

References

1. Anderson, JR. The dynamics of rhinoplasty. Presented at the Ninth International Congress in Otorhinolaryngology; August 10–14, 1969; Mexico City, Mexico.
2. Tardy, ME., Brown, R. Surgical Anatomy of the Nose. New York, NY: Raven Press; 1990.
3. Anderson JR. A plan of nasal tip surgery. Eye Ear Nose Throat Mon. 1962; 41:809–813. [PubMed: 14012866]
4. Beaty MM, Dyer WK II, Shawl MW. The quantification of surgical changes in nasal tip support. Arch Facial Plast Surg. 2002; 4(2):82–91. [PubMed: 12020201]
5. Dobratz EJ, Tran V, Hilger PA. Comparison of techniques used to support the nasal tip and their long-term effects on tip position. Arch Facial Plast Surg. 2010; 12(3):172–179. [PubMed: 20479433]
6. Gassner HG, Remington WJ, Sherris DA. Quantitative study of nasal tip support and the effect of reconstructive rhinoplasty. Arch Facial Plast Surg. 2001; 3(3):178–184. [PubMed: 11497502]
7. Willson TJ, Swiss T, Barrera JE. Quantifying Changes in Nasal Tip Support. JAMA Facial Plast Surg. 2015; 17(6):428–432. [PubMed: 26379117]

8. Carron MA, Zoumalan RA, Pastorek NJ. Measured gain in projection with the extended columellar strut-tip graft in endonasal rhinoplasty. JAMA Facial Plast Surg. 2013; 15(3):187–191. [PubMed: 23450340]
9. Janeke JB, Wright WK. Studies on the support of the nasal tip. Arch Otolaryngol. 1971; 93(5):458–464. [PubMed: 5554881]
10. Koike T, Wada H, Kobayashi T. Modeling of the human middle ear using the finite-element method. J Acoust Soc Am. 2002; 111(3):1306–1317. [PubMed: 11931308]
11. Vampola T, Laukkanen AM, Horácek J, Svec JG. Vocal tract changes caused by phonation into a tube: a case study using computer tomography and finite-element modeling. J Acoust Soc Am. 2011; 129(1):310–315. [PubMed: 21303012]
12. Gan RZ, Feng B, Sun Q. Three-dimensional finite element modeling of human ear for sound transmission. Ann Biomed Eng. 2004; 32(6):847–859. [PubMed: 15255215]
13. Lee SJ, Liong K, Lee HP. Deformation of nasal septum during nasal trauma. Laryngoscope. 2010; 120(10):1931–1939. [PubMed: 20824645]
14. Lee SJ, Liong K, Tse KM, Lee HP. Biomechanics of the deformity of septal L-Struts. Laryngoscope. 2010; 120(8):1508–1515. [PubMed: 20564665]
15. Oliaei S, Manuel C, Protsenko D, Hamamoto A, Chark D, Wong B. Mechanical analysis of the effects of cephalic trim on lower lateral cartilage stability. Arch Facial Plast Surg. 2012; 14(1):27–30. DOI: 10.1001/archfacial.2011.1354 [PubMed: 22250265]
16. Kim JH, Hamamoto A, Kiyohara N, Wong BJ. Model to estimate threshold mechanical stability of lower lateral cartilage. JAMA Facial Plast Surg. 2015; 17(4):245–250. DOI: 10.1001/jamafacial.2015.0255 [PubMed: 25927180]
17. Manuel CT, Leary R, Protsenko DE, Wong BJ. Nasal tip support: a finite element analysis of the role of the caudal septum during tip depression. Laryngoscope. 2014; 124(3):649–654. [PubMed: 23878007]
18. Shamouelian D, Leary RP, Manuel CT, Harb R, Protsenko DE, Wong BJ. Rethinking nasal tip support: a finite element analysis. Laryngoscope. 2015; 125(2):326–330. [PubMed: 25130506]
19. Conderman C, Kinzinger M, Manuel C, Protsenko D, Wong BJ. Mechanical analysis of cartilage graft reinforced with PDS plate. Laryngoscope. 2013; 123(2):339–343. [PubMed: 22965809]
20. Ortiz-Monasterio F, Olmedo A, Oscoy LO. The use of cartilage grafts in primary aesthetic rhinoplasty. Plast Reconstr Surg. 1981; 67(5):597–605. [PubMed: 7232580]
21. Mckinney, PW. The two essential elements for planning tip surgery in primary and secondary rhinoplasty: observations based on review of 100 consecutive patients. In: Miller, SH.Bartlett, SP.Garner, WL., et al., editors. Yearbook of Plastic and Aesthetic Surgery. Saint Louis, MO: Elsevier, Health Sciences Division; 2006. p. 119-120.

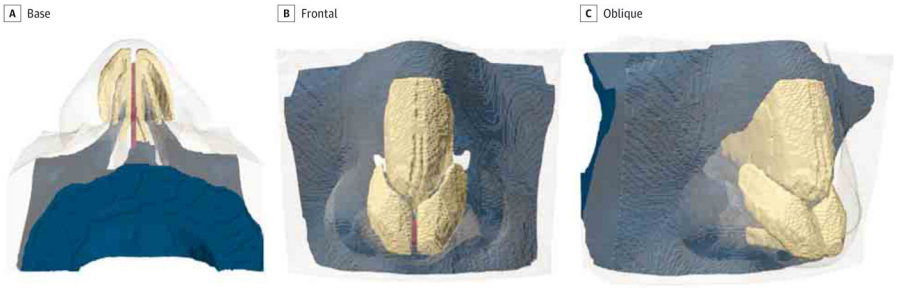

Figure 1. Control Finite Element Columellar Strut Graft (CSG) Model

A, Base view of the CSG (red) placement in between alar cartilages (white). B, Frontal view. C, Oblique view. The cartilage, skin, and CSGs in all 3 panels were drawn using Materialise Mimics software (Materialise NV), and the images rendered in COMSOL Multiphysics (COMSOL Inc).

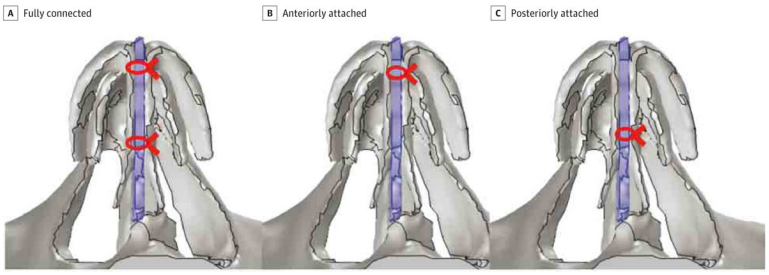

Figure 2. Schematic of Strut Placement (Purple) With Regard to the Alar Cartilages

A, Fully connected columellar strut graft (CSG) directly connected to the alar cartilages. B, Anteriorly attached CSG. C, Posteriorly attached CSG. Anterior and posterior attachments (red) were determined by where the graft connected to the alar cartilage in relation to the middle point of the nasal septum.

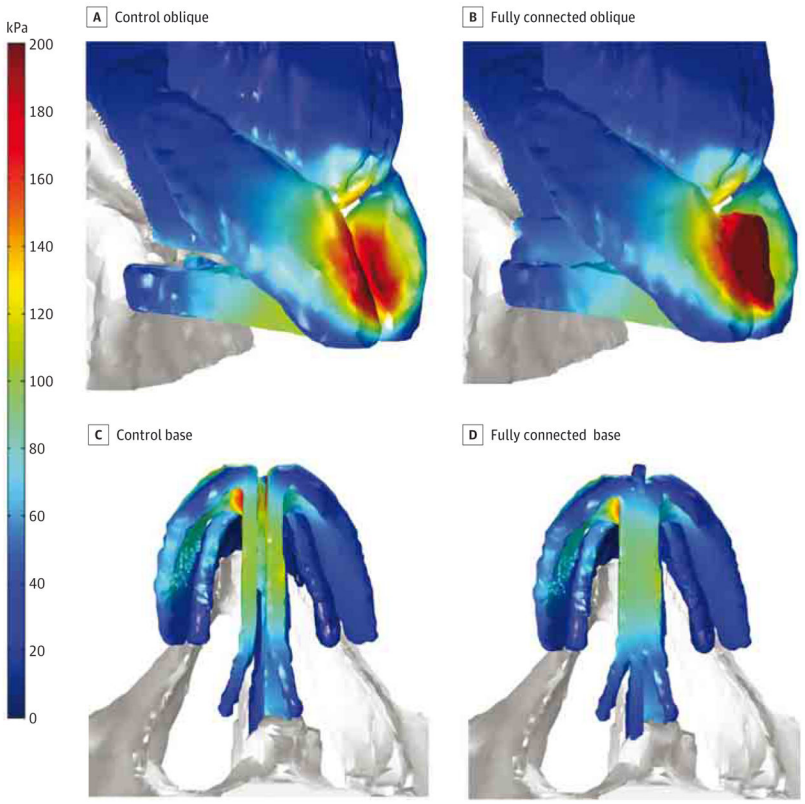

Figure 3. Surface Plot of von Mises Stress of the Cartilage Illustrated in the Oblique and Base Views of the Nose Models

A, Control (no strut) oblique view. B, Fully connected 25 × 8 × 1-mm columellar strut graft (CSG) oblique view. C, Control base view. D, Fully connected 25 × 8 × 1-mm CSG base view. The areas of red indicate high amounts of stress, while the areas in blue indicate low amounts of stress; other colors depict the intervening spectrum of stress levels. Values are represented in kilopascals.

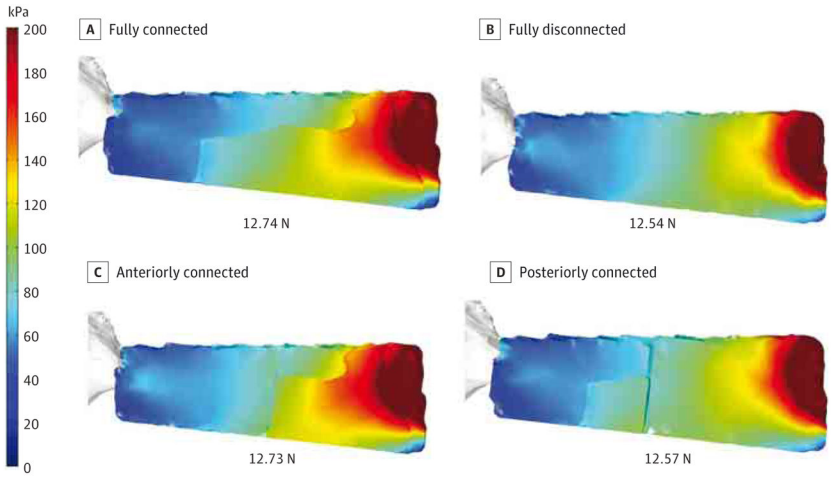

Figure 4. Surface Plot of von Mises Stress of the 25 × 8 × 1-mm Columellar Strut Graft

The areas of red indicate high amounts of stress, while the areas in blue indicate low amounts of stress; other colors depict the intervening spectrum of stress levels. Values are represented in kilopascals on the scale and Newtons beneath each image.

Table 1

Mechanical Properties of the Soft Tissue Used to Construct the Finite Element Model[a]

Mechanical Property	Skin	Cortical Bone	Cartilage
Density, kg/m^3	980	1900	1080
Yong modulus, MPa	0.5	15 000	0.8
Poisson ratio, MPa	0.33	0.22	0.15

[a]First described by Manuel et al.[17]

Table 2

Columellar Strut Graft Characteristics

Strut Dimensions, mm (Volume, mm^3)[a]	Reaction Force, N	Strain Energy Density, mJ
Control (no strut)	12.42	5.04
15 × 4 × 1 (60)	12.46	5.03
21 × 4 × 1 (84)	12.48	4.92
23 × 4 × 1 (92)	12.51	4.95
25 × 4 × 1 (100)	12.55	4.94
23 × 8 × 1 (184)	12.65	4.89
25 × 8 × 1 (200)	12.74	4.98
15 × 4 × 1 fully disconnected	12.43	5.03
25 × 8 × 1 fully disconnected	12.54	4.92
25 × 8 × 1 anteriorly connected	12.73	4.94
25 × 8 × 1 posteriorly connected	12.57	4.93

[a]The fully connected struts are organized by strut volume. In general, as the overall volume of the strut increases, so does the reaction force, measured in Newtons.